
PIV Recording Techniques

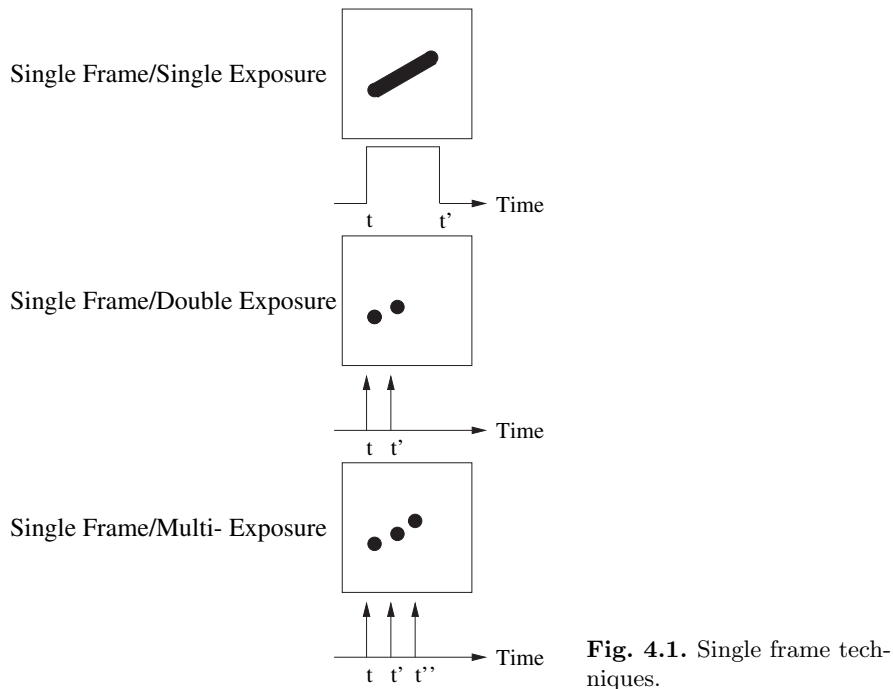
In this chapter different approaches to PIV recording are introduced. It is important to realize that the various recording methods are not necessarily defined by the recording medium. The same approach may for instance be applied using either photography or digital recording. The PIV recording modes can be classified into two main categories: (1) methods which capture the illuminated flow on to a single frame and (2) methods which provide a single illuminated image for each illumination pulse. These branches are referred to as *single frame/multi-exposure* PIV (figure 4.1) and *multi-frame/single exposure* PIV (figure 4.2), respectively [31].

The principal distinction between the two categories is that the former method, without additional effort, does not retain information on their temporal order of the illumination pulse giving rise to a directional ambiguity in the recovered displacement vector. This necessitated the introduction of a wide variety of schemes to account for the directional ambiguity, such as displacement biasing, the so-called image shifting (i.e. using a rotating mirror or birefringent crystal), pulse tagging or color coding¹ [57, 86, 91, 93, 98, 99].

In contrast, multi-frame/single exposure PIV recording inherently preserves the temporal order of the particle images and hence is the method of choice if the technological requirements can be met. Also in terms of evaluation this approach is much easier to handle.

Historically single frame/multi-exposure PIV recording was first utilized in conjunction with photography. Although multiple frame/single exposure PIV recording is possible using high-speed motion cameras, other problems such as interframe registration arise. Continual development over the past decade in the area of electronic imaging has made multi-frame/single exposure PIV recording possible at flow velocities extending into the hypersonic domain.

¹ Strictly speaking color coding is a form of *multi-frame/single exposure* PIV: the color recording can be separated into different color channels containing single exposed particle images.



This chapter on PIV recording is organized as follows: after an introduction to the cameras most frequently used, the advantages and associated problems of single frame recording and image shifting will be discussed. The second part will introduce multiple frame PIV recording mainly in the context of digital imaging.

A description of all possible recording techniques that can be used for PIV cannot be given here. A variety of different sophisticated ideas related to this problem has been reported in the literature over the past few years, most of them with special advantages for individual applications. It is clear that a decision on which method is best cannot be made without taking the individual needs of each application into account. Therefore, the recording techniques described here are not complete and not necessarily the best, but the most common.

In summary it can be said that the design of an experimental setup for PIV is based on a decision of which of the following goals have priority:

- high spatial and/or temporal resolution of the flow field under investigation,
- the required resolution of velocity fluctuations,
- the time interval between the individual PIV measurements, and
- which components are already available in the laboratory or can be obtained at adequate costs.

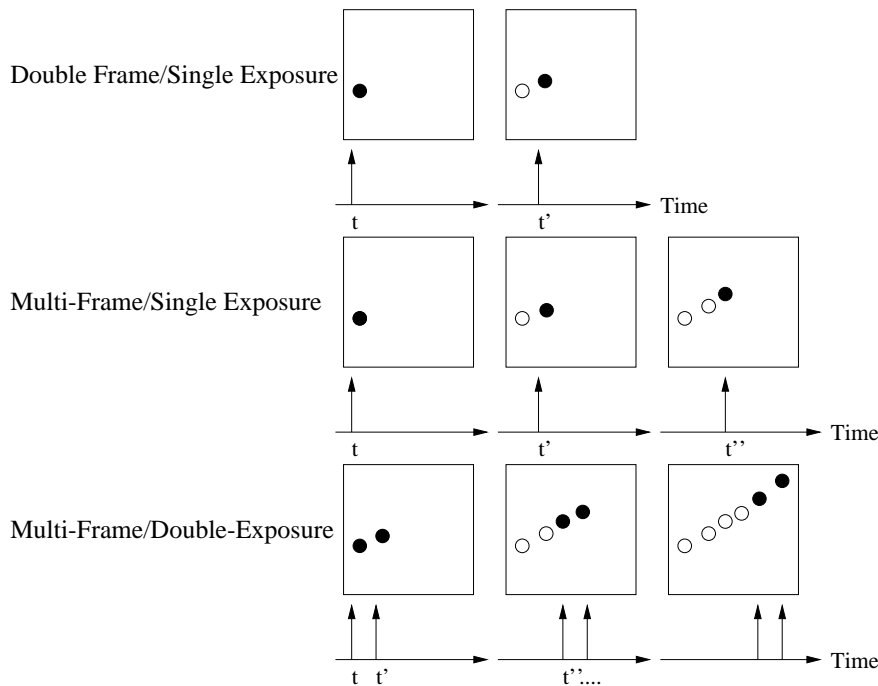


Fig. 4.2. Multiple frame techniques (open circles indicate the particles' positions in previous frames).

Depending on the choice of priority an appropriate system for recording can be configured. However, it must be kept in mind that not every requirement can be fulfilled, which is mainly due to technical limitations such as the available laser power, pulse repetition rates, camera frame rate, etc. The selection of the recording system also influences the method for directional ambiguity removal and, hence, the evaluation technique to be used. Today, photographic recording and mechanical image shifting – which have been used for a long time because of the obtained quality of the recordings – might not be considered the first choice anymore. Video recording offers so many advantages by allowing for immediate feedback and quality optimization during the course of the experiment. This is of high interest for most applications, especially with a view to operational costs.

4.1 Film Cameras for PIV

The current level of technology allows digital recording to achieve a high spatial resolution that can be compared with that of 35 mm film cameras. However, especially if using large format films, resolutions can be obtained which are more than one order of magnitude larger than that of digital cameras. The

photographic technique is a method of choice for PIV applications requiring high spatial resolution without peak-locking. One major disadvantage of the photographic technique is that it is difficult to record the images of the tracer particles on to different frames, especially in the case of high-speed investigations where pulse separation times, of the order of a few microseconds are required. This indicates that the problem of directional ambiguity removal has to be solved for photographic PIV in a reliable and flexible manner using a technique such as image shifting which will be described below.

4.1.1 Example of a PIV Film Camera

Initial PIV experiments have shown that a high quality and reliable focusing device is necessary, in order to save time in the alignment of the system. For this purpose a photographic camera should be equipped with a device for fast focusing. A small area in the film plane can for example be observed by means of a CCD camera looking through an orifice in the back wall of the camera in order to control focusing[58]. This focusing device worked well and helped to reduce the time necessary for alignment considerably. A different solution which possesses some technical advantages has been suggested in the literature [60, 68].

A low cost standard CCD sensor mounted in the viewfinder of a single-lens reflex (SLR) photo camera can be used for fast and reliable focusing (figure 4.3). The position of the CCD sensor has to be carefully aligned in such a way that the distance between the lens and the CCD sensor via the mirror is exactly the same as that from the lens to the film plane. The distance between the light sheet and the film plane can be changed by moving the complete camera system by means of a traversing table, thereby observing for minimum particle image diameters on a monitor.

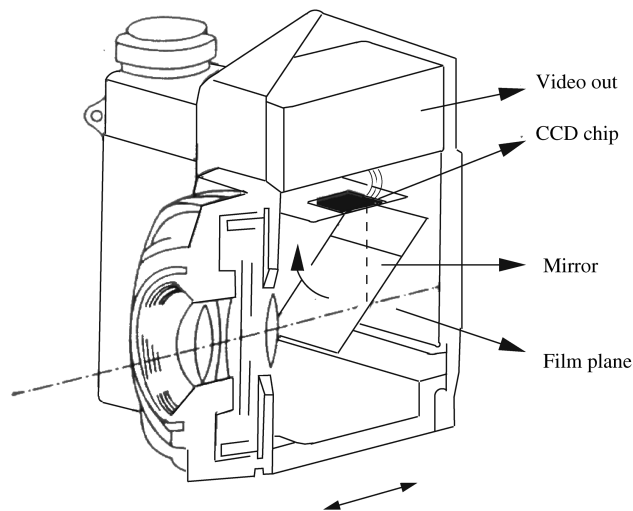


Fig. 4.3. Photo camera with CCD sensor for fast focusing.

4.1.2 High-Speed Film Cameras

The first high-speed cameras have already been developed shortly before and more intensively during the second world war [96]. First developments consisted of standard components to which a motorized fast drive had been coupled, which rapidly moved the film from one roll to the other. Rotating prisms generated a synchronized periodic shift of the projected image in order to allow for longer exposure times. The limiting factors for those solutions are the acceleration forces and the mechanical film properties. The maximum frame rates of those cameras are approximately 1000 frames/s.

Much higher frame rates can be obtained by drum cameras. They consist of a rotating mirror on which the image is projected by the primary object lens as shown in figure 4.4. The mirror has an inclination of 45° with respect to the axis of rotation. A couple of secondary lenses around the rotating mirror projects the image onto the photographic film, which is attached to the inner wall of the cylinder around the mirror. Some major technical problems had to be solved for this type of camera in order to reach the current state of technology. First, a motor had to be coupled which offers a high acceleration before the recording and a high and constant speed during recording. Second, resonances causing inner vibrations and high structural loads during the acceleration and constant revolution had to be avoided. And third, highly complex electro-mechanical or electro-optical shutters were required.

Even if high-speed drum cameras have not been developed much further over the past decade, their frame rates of up to 10^7 frames/s together with the high spatial resolution of photographic material makes them superior with respect to modern high-speed digital cameras. Only the costs of multiple oscillator lasers that would allow such high pulse rates and their complicated handling prevent them to be used in many applications.

4.2 Digital Cameras for PIV

Over the last decade, CCD based digital cameras, as described in the following sections, became the work horses for nearly all technical and scientific PIV applications that required only moderate or no temporal resolution. Flash lamp pumped double oscillator Nd:YAG-lasers offer high pulse energies and

Fig. 4.4. Sketch of a high-speed photographic drum camera.

repetition rates that matched with the frame rates of most of the commercially available CCD cameras. The CCD cameras offer two important advantages, one being increased spatial resolution, the second the electronic architecture that permits two PIV recordings, temporally spaced by microseconds, by the same camera (see 4.2.4). Therefore, the CCD sensors will be described in considerable detail in the following.

In section 2.8 the CCD as an imaging sensor was described. Next the various types of CCDs are introduced in the context of application to PIV recording. Figure 4.5 schematically describes the layout of a CCD sensor. The individual pixels are typically grouped into a rectangular array to form a light sensitive area (linear, circular or hexagonal formats also exist). It should be pointed out that, in contrast to most CMOS sensors, in CCD sensors the pixels in the array cannot be randomly addressed the way memory can be addressed in a computer. Rather, the array has to be read out sequentially in a two-step process: after exposing the sensor the accumulated charge (i.e. electrons) is shifted vertically, one row at a time, into a masked-off analog shift register on the lower edge of the sensor's active area. Each row in the analog shift register is then clocked, pixel by pixel, through a charge-to-voltage converter and thereby provides one voltage for each pixel. The stream of pixel voltages along with a variety of synchronization pulses compose the actual (analog) video signal. Depending on the employed image transmission format the read-out of the sensor can either be sequential (also known as *progressive scan*) or interlaced, in which first all odd rows are read out before the even rows are accessed. The latter is the common format for standard video equipment (see also section 2.10). Since the progressive scan approach preserves the image integrity, it is more useful for PIV recording as well as for other imaging applications such as machine vision.

In the following four sections we will concentrate on the operation of the various types of CCD sensors and how these may be utilized in PIV recording. Section 4.2.5 deals with the recently developed active pixel CMOS sensors, which became the state of the art design of sensors used for high-speed PIV. Sections 4.2.6 and 4.2.7 describe camera types that can be used for high-speed recording, whereas sections 2.9 and 4.4.1 should be consulted in regard to the utilization of standard (consumer) video equipment for PIV recording. A short summary of the features of digital cameras that are considered to be essential for PIV is given in section 2.8.1.

4.2.1 Full-Frame CCD

The full-frame CCD sensor represents the CCD in its classical form (figure 4.5): a photosensitive area of pixels that is first exposed to light and then read out sequentially (progressive scan) on a row-by-row basis without separating the image into two separate interlaced fields such as in standard

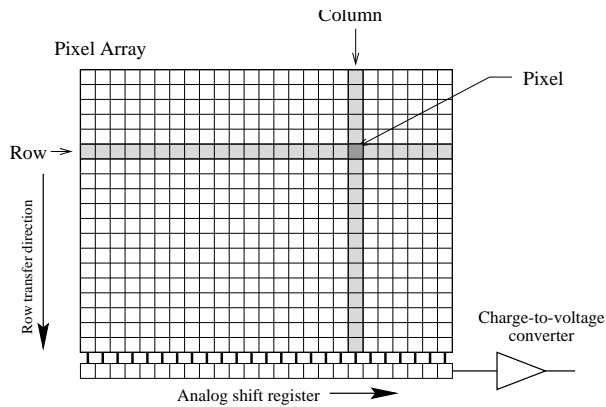


Fig. 4.5. Typical CCD sensor geometry.

video. This sensor has been in use in scientific imaging such as astronomy, spectroscopy and remote sensing ever since its introduction in the 1960's. It is characterized by large fill factors which can even reach 100% for special back-thinned, back-illuminated sensors². With adequate cooling and slow read-out speeds, imaging at very low noise levels with high dynamic range (up to 16 bits) is possible. The most striking advantage is that these sensors are available as very large arrays with pixel counts exceeding tens of millions (7000×5000 pixel).

The use of these sensors does however have some major drawbacks. To achieve the low read-out noise and high dynamic range, the pixel read-out rate has to be kept low. Even at standard video characteristics the data rate is limited to 10 – 20 MHz which results in a decreasing frame rate as the number of pixels increases. Frame rates of less than 1 Hz are not uncommon for larger sensors. For this reason multiple read-out ports are sometimes used, which brings about the problem of calibrating the respective charge-to-voltage converters with respect to one another. Another drawback is that the sensor stays active during read-out. Unless a shutter is placed in front of it, light falling on to the sensor will also be captured resulting in a vertical smear in the final image.

Because of its high spatial resolution, the full-frame sensor can be used as a direct replacement of photographic film. These sensors are frequently incorporated into 35 mm SLR camera bodies. As for their use in PIV, single images containing multiple exposed particle images ($n_{\text{exp}} \geq 2$) can be recorded analogous to the photographic method. The same ambiguity removal schemes as in photographic PIV recording (rotating mirror, birefringent crystal) can be employed. If the flow under investigation is sufficiently slow in comparison to the frame rate of a camera based on this sensor, then single exposed PIV

² In case of a back-illuminated CCD, the photo-active parts are illuminated from “behind” through the silicon-substrate. Therefore, the back of the device is thinned down to $O[10] \mu\text{m}$ and coated to avoid reflexions.

recordings can be obtained. In this case the ambiguity removal schemes are not needed. The timing charts given in figure 4.9(a) and (b) summarize how the particle illumination pulses have to be placed to produce single exposed or multiple exposed PIV images.

4.2.2 Frame Transfer CCD

The pixel architecture of the frame transfer CCD sensor (figure 4.6) is essentially equivalent to that of the full-frame CCD sensor with the difference that the lower half of its rows are masked off and cannot be exposed by incoming light. Once exposed, the rows of accumulated charge are rapidly shifted down into the masked-off area at rates as fast as $\Delta t_{\text{row-shift}} = 1 \mu\text{s}$ per row. The entire image can thereby be shielded from further exposure within $\Delta t_{\text{transfer}} = 0.5 - 1 \text{ ms}$ depending on the vertical clocking speed and vertical image size. However, the sensor does stay active during the vertical transfer time such that vertical smear is possible. Charge stored within the masked area prior to the shift is lost however. Once the shift has been completed, the sequential read-out is equivalent to that of a full-frame CCD.

The frame transfer CCD sensor offers two application possibilities in PIV recording. The fast transfer of the accumulated charge into the storage area allows two single exposed PIV images to be captured at a time delay, Δt , slightly longer than the transfer time, for example $\Delta t \geq \Delta t_{\text{transfer}}$. To achieve this, the illumination pulses are placed such that the first pulse occurs immediately before the frame transfer event (i.e. on frame n), while the second pulse occurs immediately thereafter (i.e. on frame $n + 1$, see figure 4.9(c)).

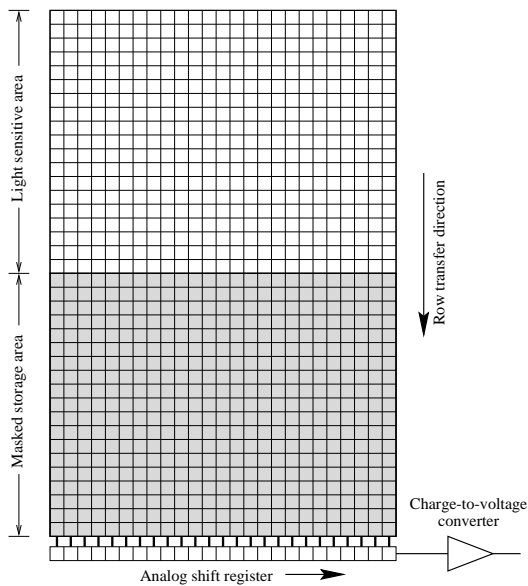


Fig. 4.6. Frame transfer CCD sensor layout.

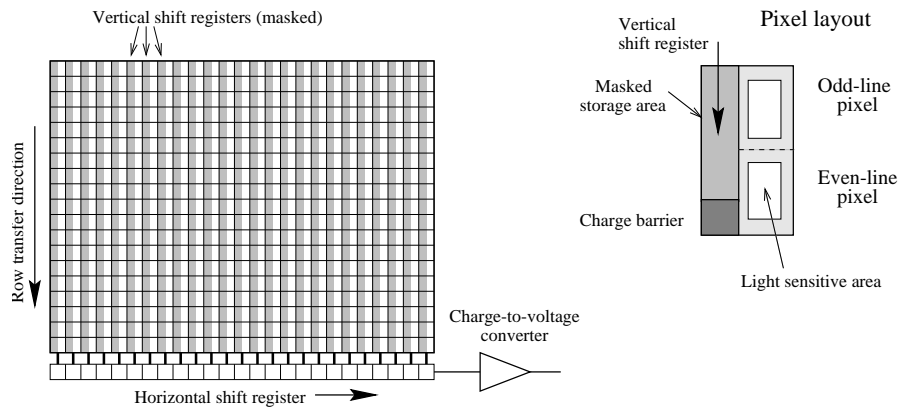


Fig. 4.7. Interline transfer CCD layout.

This placement of the illumination pulses with respect to the CCD sensor's periodic exposure cycles is sometimes referred to as *frame straddling*. At standard video resolution and a field of view of 20 cm the measurement of flow velocities up to the order of 5 m/s is possible. In this case the PIV frame rate is half the camera frame rate (e.g. 15 Hz for NTSC video, 12.5 Hz for PAL video).

The frame transfer CCD sensor can alternatively be used to impose an image shift in order to remove the displacement bias associated with double exposure single frame PIV recording. This is achieved by placing the first illumination pulse just prior to the start or at the beginning of the vertical transfer period (figure 4.9(d)). The second light pulse is placed such that it occurs while the collected charge of the first exposure is transferred into the masked area. For example, at a transfer rate of $\Delta t_{\text{row-shift}} = 1 \mu\text{s}$ per row, a pulse delay of $\Delta t = 10 \mu\text{s}$ would produce a maximum of 10 pixel image shifts. In this mode of operation the PIV frame rate is equal to the camera's frame rate. In this context it should be mentioned that standard CCD sensors are also capable of performing this type of displacement biasing [113].

4.2.3 Interline Transfer CCD

The interline transfer CCD sensor takes its name from additional vertical transfer registers located between the active pixels. Typically two vertically adjacent pixels share a common storage site in the vertical shift registers as shown on the right of figure 4.7.

Charge accumulated in the active area of the pixel can be rapidly transferred into the storage area ($\Delta t_{\text{transfer}} < 1 \mu\text{s}$). This fast charge dumping feature also opens the possibility for full electronic shuttering on the sensor level. This type of sensor is among the most common in consumer video

products and hence readily available at standard video resolutions (see also table 2.9) although high resolutions are also in use. Contrary to the previously described framing CCD sensors, the interline transfer CCD sensor tends to be more sensitive in the blue-green region of the light spectrum (see figure 2.49).

The major drawback of these sensors is their reduced fill factor due to the additional storage sites next to each light-sensitive area. Additional microlenses on the face of the sensor improve their light gathering capability. The alternative back-thinning approach is not possible with this sensor due to the additional storage sites which have to stay shielded against light exposure.

Since the sensor only provides half as many charge storage sites as there are active pixels, an image can only be stored at half the vertical resolution. This storage mode is an artifact of standard video transmission which separates a full image frame into distinct *fields* containing only even or odd lines (see section 2.10). Thus, the sensor can offer only half the vertical resolution in the shuttered mode of operation. For example if the odd lines of captured image data are read out from the sensor, the even lines are accumulating charge and vice versa. As a result, the odd and even lines are active during different periods of time, resulting in the capture of image data that is staggered by the period of one field for adjoining video lines – captured images of moving objects seem to flicker back and forth.

Cameras based on the interline transfer CCD have two possible applications in electronic PIV recording. The electronic shutter can be used to shutter the light of a continuous wave laser such as an argon-ion laser (figure 4.9(e)). This electronic shutter is implemented by means of a clamping voltage on each pixel which inhibits the photon-to-charge conversion of the CCD for most of the framing interval; leaving a short period for photon collection just prior to the charge transfer event. Since the temporal position of the light-sensitive period is fixed relative to the camera's field rate, the effective pulse delay, Δt , will be equivalent to the field rate (e.g. $\Delta t = 20$ ms for CCIR, $\Delta t = 16.7$ ms for NTSC). This limits the application to low-speed phenomena which can however be resolved in time.

In the second mode of operation the electronic shutter has to be completely deactivated making the sensor active at all times except for the brief charge transfer event. The illumination is provided by a pulsed laser (figure 4.9(f)). In this case the frame straddling method is applied in which the first of the two illumination pulses is placed before the transfer event and the second right afterward (see also section 4.2.2). Thereby two single exposed images with half the vertical resolution (i.e. fields) can be recorded with a very short effective pulse delay which may be as short as the 1–2 μ s duration of the charge transfer. The technique was first applied by Wernet [110] to measure a free jet in the 100 m/s range using a CW-laser and an intensified, interline-transfer CCD camera. Further implementations and applications are reported in [97, 100, 106, 111]. Since two fields comprise a frame the effective PIV image frame rate is equivalent to the camera frame rate (e.g. 25 Hz for CCIR, 30 Hz for NTSC), given that the pulse laser can provide pulse pairs at this

frequency. In this context it should be observed that PIV recording based on interlaced images is only reliable when the particle image diameter is large enough such that particle images will not disappear in the inactive scan-lines of the second exposure, and vice versa.

4.2.4 Full-Frame Interline Transfer CCD

This sensor is a derivative of the interline transfer CCD described before with the difference that each active pixel has its own storage site (figure 4.8, right side). Introduced in the first half of the 1990's cameras based on these progressive scan sensors rapidly gained popularity in the field of machine vision as they removed all the artifacts associated with interlaced video imaging. The electronic shutter can be applied to the entire image rather than to one of its fields as for standard interline transfer CCDs. Here also microlenses above each pixel help raise the effective fill factor from 20% to up to 60%.

The fast transfer of the entire exposed image into the adjoining storage sites within a few microseconds in conjunction with higher resolution formats, in a departure from the standard video resolutions, has extended the application of single exposure double frame PIV images into the transonic flow velocity domain. Here the maximum PIV image frame rate is half the camera's frame rate with pulse delays as low as $\Delta t = 1 \mu s$ [109, 112]. As these cameras also frequently have asynchronous reset possibilities, their range of application is the most flexible of the CCD systems described in this chapter. A timing diagram for PIV recording based on this sensor is given in figure 4.9(g).

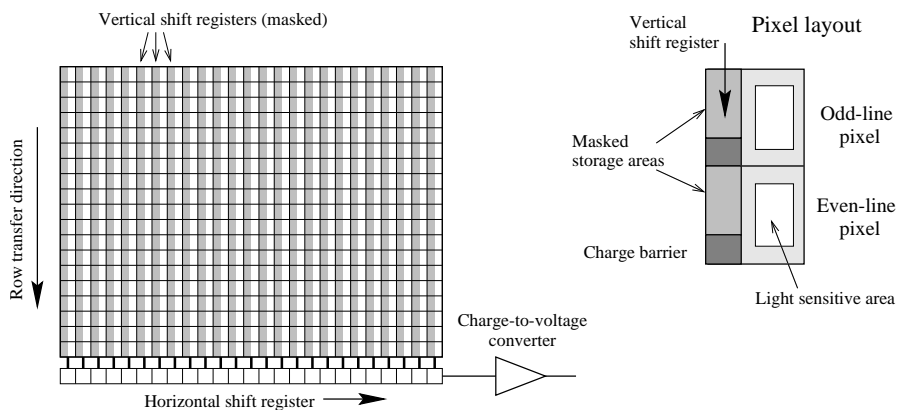


Fig. 4.8. Progressive scan, interline transfer CCD layout.

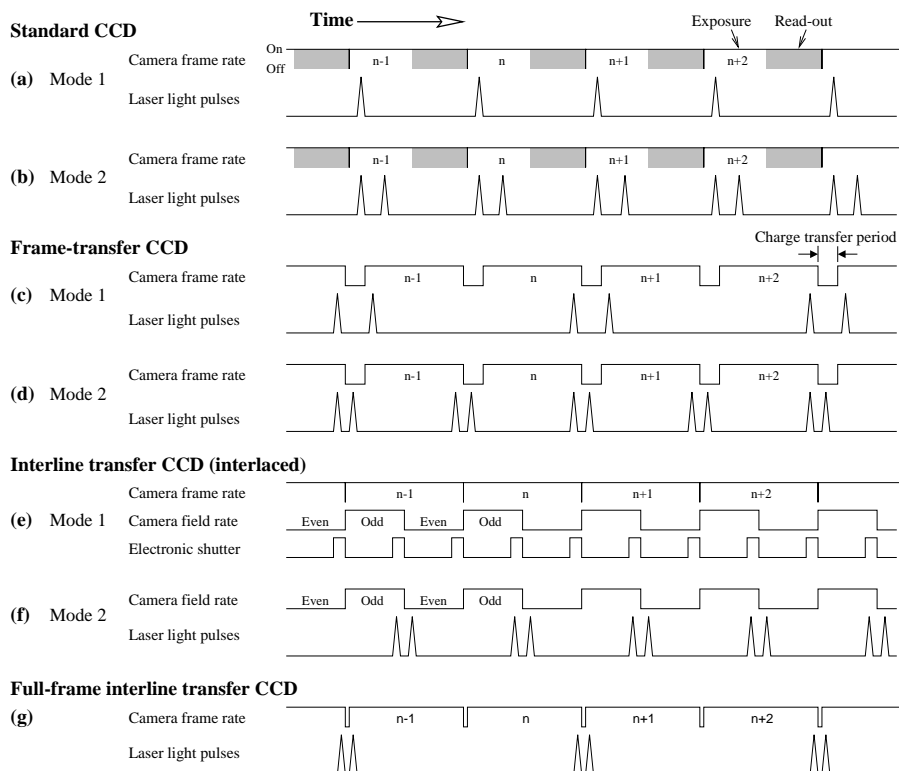


Fig. 4.9. Timing diagrams for PIV recording based on various types of CCD sensors.

4.2.5 Active Pixel CMOS Sensor

The most relevant CMOS sensors for PIV applications are based on the active pixel sensor (APS) technology in which, in addition to the photodiode, a readout amplifier is incorporated into each pixel. This converts the charge accumulated by the photodiode into a voltage which is amplified inside the pixel and then transferred in sequential rows and columns to further signal processing circuits as described in section 2.8.2. As can be seen in figure 4.10 each pixel contains a photodiode, a triad of transistors that converts accumulated electron charge to a measurable voltage, resets the photodiode and transfers the voltage to a vertical column bus. In addition to that, some CMOS sensors contain shutter transistors for each pixel. The amplifier transistor represents the input device of what is generally termed a source follower. It converts the charge generated by the photodiode into a voltage that is output to the column bus. The reset transistor controls integration time, and a row-select transistor connects the pixel output to the column bus for readout.

During the operation of the sensor, first the reset transistor is initialized in order to drain the charge from the photosensitive region. Then, the inte-

Fig. 4.10. APS-CMOS pixel layout with integrated amplifier (source follower).

gration period begins and the electrons from the photo diode are stored in the potential well lying beneath the surface. After the integration period, the row-select transistor connects the amplifier transistor in the selected pixel to its load to form a source follower and thus converts the charge of the photo-diode into a voltage on the column bus. The cyclic repetition of this process to read out every row thereby forms the image.

One problem that frequently occurs when recording PIV images close to model surfaces with CCD cameras is blooming (see section 2.8.1). In this case, the high intensity of the light scattered from the surface leads to a migration of electrons to neighboring pixels, that makes the recording of particle images in those areas impossible. One of the main advantages of most CMOS sensors is their ability to record images with high contrast without blooming.

4.2.6 High-Speed CCD Cameras

In section 4.2 the different types of CCD sensors were introduced. These sensors, especially the full-frame interline transfer CCD, is chosen for most of the conventional PIV applications with moderate frame rates. However, special developments based on the CCD technology can also be used for high-speed PIV.

High frame rates, together with the relatively high spatial resolution needed for most PIV applications result in large amount of data that has to be transferred from the chip into the storage. This required high clock speeds and, as a consequence thereof, a high bandwidth of the read out electronics. The high bandwidth of the sensor increases the noise while the efficiency decreases. Those problems resulted in sensor designs, in which the sensor is divided into smaller segments, which are read out in parallel. The required read out speed could therefore be reduced by the number of separate channels [108]. In addition to that, most of the CCD based high-speed cameras contain a so-called split-frame storage into which half of the image is read-out from the top of the chip and the other half from the bottom. In spite of all the efforts to increase the combined pixel readout rates by parallel transfer and storage, the rates are considerably higher in comparison to conventional cameras and the read out electronics need to be carefully optimized with respect to noise.

Today's commercially available high-speed CCD cameras offer frame rates of about 1000 frames/s at moderate resolutions in the 512×512 pixel range.

4.2.7 High-Speed CMOS Cameras for PIV Recording

The most advanced high-speed cameras suitable for PIV have CMOS sensors. The parallel structure of the CMOS sensor, which has been described previously, allows more channels than were practical with CCDs. CMOS cameras used for high-speed PIV application frequently have 32 or more output channels. For the clock speed CMOS cameras offer higher pixel rates, since CMOS pixels can be read out with one clock pulse, while CCDs typically require two to four clock pulses per pixel read out. In contrast to most CCD sensors, high-speed CMOS sensors have electronic shuttering integrated in each pixel. As already mentioned, CMOS sensors are not prone to blooming. While saturation effects can occur, high pixel intensities do not effect the image in the way blooming in CCD sensors does. Windowing, the formerly described technique to read smaller sub windows of the CMOS sensor array, is a feature that allows to produce higher frame rates at reduced image resolutions. This feature is available in most of the high-speed CMOS cameras and frequently used for high-speed PIV recording, since it allows for using the very high repetition rates of most high-speed lasers. Some CMOS cameras allow an extremely flexible read-out of the sensor. They may have hundreds of selectable resolutions, helping the user to obtain the desired resolution at maximum performance. Advanced CMOS-sensor designs use fewer components per pixel than earlier designs and take advantage of smaller size of the components. This leads to a better light sensitivity than that of most CCD based high-speed cameras. Additionally, the image quality of new CMOS high-speed cameras has significantly been improved. And the fact that some leading manufactures of digital SLR cameras nowadays offer CMOS sensors in these products, leads to the assumption that this trend is continuing.

Today's commercially available high-speed CMOS cameras offer frame rates exceeding 3000 frames/s at full mega pixel resolution. At 512×512 pixel resolution they even reach 10,000 frames per second. In order to save the enormous amount of data, that can be recorded within seconds with such a performance, many cameras have memory of up to 16 GB on board where data are stored prior to transfer to the computer.

4.3 Single Frame/Multi-Exposure Recording

When using photographic film or single frame digital cameras for PIV recording, two or more exposures of the same particles are stored on a single recording. Therefore, the sign of the direction of the particle motion within each interrogation window cannot be determined uniquely, since there is no way to

decide which image is due to the first and which is due to the second illumination pulse. Although, for many applications the sign of the velocity vector can be derived from a priori knowledge of the flow, other cases involving flow reversals, such as in separated flows, require a technique by which the sign of the displacement can be determined correctly.

4.3.1 General Aspects of Image Shifting

The great interest in PIV measurements in many different fields of research requires a flexible technique for ambiguity removal that can be applied to a variety of experimental situations. Especially for aerodynamic investigations it is very important to be able to apply this technique to high-speed flows, that is with short time intervals of the order of a few microseconds between the exposures. One method is the image shifting technique as described by various authors [86, 89, 98] that removes the directional ambiguity. Image shifting enforces a constant additional displacement on the image of all tracer particles at the time of their second illumination. In contrast to other methods for ambiguity removal, which require a special, or at least a specially adapted, method of evaluation, image shifting leaves the proven evaluation process employing statistical methods unchanged.

Elimination of the ambiguity of direction: Figure 4.11 explains the removal of directional ambiguity of two tracer particles by means of image shifting, one of which is moving to the right and the other one is moving to the left (flow reversal). Introducing an additional image shift, d_{shift} , to the flow-induced displacements of the particle images d_1 and d_2 , the situation changes. By a selection of the additional image shift, d_{shift} , in such a manner that it is always greater than the maximum value of the reverse-flow component (i.e. d_2), it is guaranteed that the tracer images of the second exposure are always located in the “positive” direction with respect to the location of the first exposure (figure 4.11). The elimination of the directional ambiguity does not depend on the direction within the observation plane where the shift takes place if the maximum of the corresponding reverse-flow component is predicted accordingly. Thus, an unambiguous determination of the sign of the displacement vector is established. The value and correct sign for the displacement vectors d_1 and d_2 will be obtained by subtracting the “artificial” contribution d_{shift} after the extraction of the displacement vectors for the PIV recording.

4.3.2 Optimization of PIV Recording for Autocorrelation Analysis by Image Shifting

As already mentioned in chapter 3 the application of the cross-correlation technique for two subareas of a single frame/multi-exposure recording instead of performing an autocorrelation on a single subarea, increases the flexibility of the PIV system. This evaluation approach cannot remove the directional ambiguity of the velocity vectors or handle situations where the image

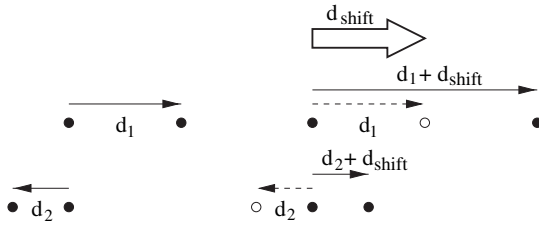


Fig. 4.11. Elimination of the ambiguity of direction of the displacement vector as observed in the recording plane.

displacements are of the order of the particle image diameter. However, the pulse separation time can be adapted in a wider range, because the size of the two interrogation windows and their displacement can be adapted later on during evaluation.

If the evaluation system is not flexible enough to allow cross-correlation of slightly displaced interrogation areas, the evaluation process of doubly exposed PIV recordings has to be analyzed by autocorrelation. This problem often occurred in the past when optical evaluation was used in order to improve the signal-to-noise ratio. Besides resolving the directional ambiguity, image shifting is required in order to optimize the recording for later autocorrelation evaluation. More details on the different aspects of image shifting were described by RAFFEL & KOMPENHANS [104]

4.3.3 Realizations of Image Shifting

The most widely used experimental technique for image shifting involves the use of a rotating mirror over which the observation area within the flow is imaged on to the recording area in the camera. The magnitude of the additional displacement of the images of the tracer particles depends on the angular speed of the mirror, the distance between the light sheet plane and the mirror, the magnification of the imaging system and the time delay between the two illumination pulses [98]. Various experimental setups employing rotating mirrors were realized by different authors and have shown good experimental results, such as the investigation of dynamic flow separation (wake with flow reversals) above profiles [61].

In order to achieve very high shift velocities, electro-optical methods employing differently polarized light for illumination have been proposed and applied by LANDRETH & ADRIAN [99], LOURENÇO [101] and MOLEZZI & DUTTON [64]. The constant shift of the particle images is obtained by means of birefringent crystals of appropriate thickness. REUSS describes the problems associated with this method, such as “depolarization effects” [105].

Another scheme by which the directional ambiguity problem may be resolved has been presented by WORMELL & SOPCHAK and involves a CCD camera in which the charge associated with the first illumination is electronically moved by a known distance within the sensor during the time period between the first and the second laser pulse [113] (see section 4.2.2). This

arrangement allows a minimum pulse separation of approximately $40 \mu\text{s}$. At DLR many successful applications have been performed with a rotating mirror system for image shifting. A detailed description of such a system, is given below.

A rotating mirror based image shifting system has the following advantages: it can easily be implemented into already existing apparatus for employing single frame/multi exposure recordings; it makes no additional demands on the scattering characteristics of the particles (light depolarization effects can be neglected); the shift velocity can be adapted to the problem very easily; and a much higher shift velocity can be attained than by moving the entire camera.

It should be mentioned here that the rotating mirror technique is limited by a maximum frame rate which is given by the product of the angular speed and number of mirror surfaces. In most aerodynamic applications the maximum framing rate is higher than the repetition rate of a standard pulse laser system. Nevertheless, the framing rate may become a limiting factor, for example, when flow fields are observed at low flow (and shift) velocities with high resolution in time. Furthermore, it is not possible to synchronize non-periodic flow events with a mirror that is rotating at a constant speed.

4.3.4 Layout of a Rotating Mirror System

Figure 4.12 shows the high-speed rotating mirror system for image shifting as used at DLR in Göttingen. It allows shift velocities exceeding 500 m/s without any noticeable reduction of the optical quality of the images.

The system shown in figure 4.12 consists of the following components: a shaft mounted in precision bearings, a mirror mount attached to one end of the shaft and an optical encoder connected to the other end. The mirror assembly is driven by a stepper motor with stable revolution frequencies ranging from 1 to 100 Hz. A toothed belt guarantees slip free transmission while a revolving mass attached to the rotating shaft compensates for the velocity fluctuations of the motor drive. The optical encoder is a commercially available angle encoder that is coupled to the shaft using a twist free shaft clutch and supplies the signals for the laser triggering as well as angular frequency monitoring. This precisely machined setup ensures that the 90° angle required between objective lens and observation plane is exactly reproducible even in a noisy industrial environment.

The adaption of the signal frequency from the angle encoder to the repetition rate of the pulse laser is performed by digital dividers, see figure 4.13. The angular position of the mirror at the time of image capture is kept constant by means of a digital controller and is phase-locked to the trigger for the laser pulses. The controller itself was designed in such a manner that it is able to handle severe electronic noise due to the stepper motors or the electric drive systems present in many wind tunnel environments. The procedure

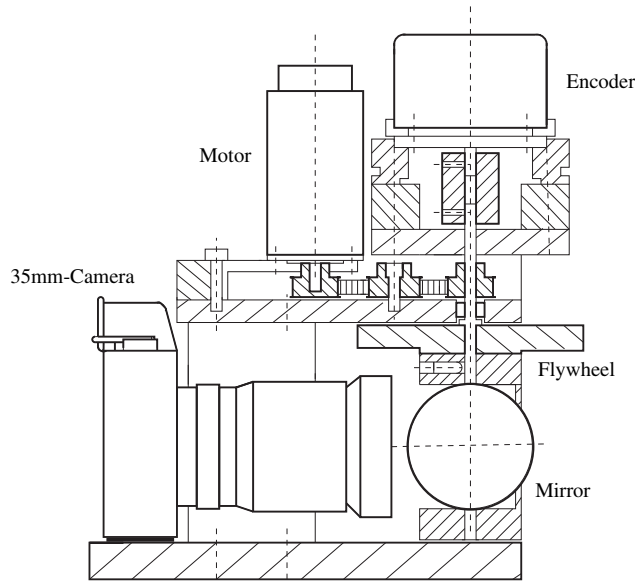


Fig. 4.12. Schematic diagram of the rotating mirror system.

of controlling the observation angle is as follows: Signal (*a*) is the increment signal from the encoder. The resolution of 1000 pulses per revolution as delivered by the encoder was sufficient. Signal (*b*) is the reference signal (recording position) from the encoder which usually is one inverted pulse per revolution. Signals (*a*) and (*b*) are combined by a logical AND gate in the angle controller. The resulting signal (*c*) and a signal obtained from the light pulse of the laser (*d*) are combined by a logical OR gate. This signal, (*e*), is used to control the laser and the camera for recording. If the reference signal (*b*) and the light

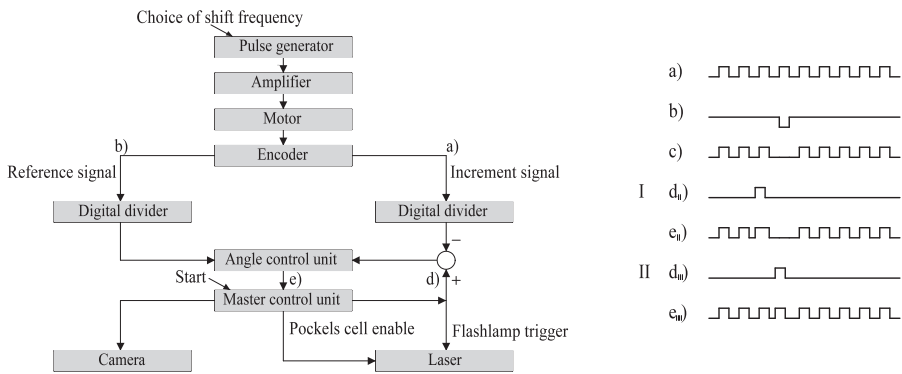


Fig. 4.13. Flow and impulse chart of the angle control.

pulse (d_I) do not coincide (Case I), different pulse rates are obtained for laser (e_I) and mirror control (a). This leads to a phase shift in each revolution until the reference signal (b) and the light pulse (d_{II}) coincide temporally. In this case (Case II) the pulse rates of the increment signal of the encoder (a) and of the control signal for the laser (e_{II}) are the same and the control error equals zero. The digital dividers included in the signal chain allow a variation of the mirror revolutions and the framing rate. The main advantage of this image shifting setup is the easy handling and the flexibility in adjusting the shift velocity, which can be chosen from a wide range in very small steps just by “pressing a button”.

This section described how to build a rotating mirror system which is precisely phase locked with the laser light pulses. However, there exist additional error sources in rotating mirror systems. In particular the way in which the virtual image of the tracer particles is moved by the rotation of the mirror has to be taken into account. It will be shown in the following that the movement of the particle images due to the rotating mirror are not uniform over the recording, but vary locally. By means of the equations arising from the system’s optical geometry derived in the following, algorithms can be implemented, which allow a full compensation of these errors.

4.3.5 Calculation of the Mirror Image Shift

In the literature, the motion of the virtual image due to the rotation of the mirror is derived from geometric relations in two dimensions with assumptions that are not valid in general [92]. Only the displacement of the depth-of-field center from the light sheet was determined in order to estimate the effect of this parameter on the defocusing of the images of the particles [103]. In most cases, the shift of the particle images d_{shift} is assumed to be constant in the entire observation area:

$$d_{\text{shift}} = 2\omega_m Z_m M \Delta t \quad (4.1)$$

where ω_m is the angular velocity of the rotating mirror, Z_m the distance between the light sheet and mirror-axis ($Z_m = \text{const.}$), M the magnification (image size/object size) and $\Delta t = t' - t$ the time delay between the light pulses. The fact that the distance between the mirror axis and a point of the virtual light sheet is not constant but a function of the x -coordinate leads to an error of equation (4.1) of more than 1% of the mean image shift at typical experimental conditions. A further, additional error results from the direction of movement of the virtual image. Since the z component of the virtual particle image shift increases towards the edges of the virtual observation area, there is also an influence on the x and y components due to the perspective projection of the virtual particle image on to the recording plane. In order to fully describe the effects of a shift component perpendicular to the virtual light sheet on the position of the image points in the coordinate system x, y, z , the imaging through the lens must also be considered.

Details on the mathematical procedure can be found in [104]. As a result the image displacement $\mathbf{d} = \mathbf{x}' - \mathbf{x}$ due to mirror rotation can be obtained (see equation (4.2) and equation (4.3)). Equation 4.1, which is given in the literature for the shift of the tracer images due to a rotating mirror, can be derived from the exact solution by the following assumptions:

- Δt approaches zero;
- the axis of rotation of the mirror lies on the optical axis;
- the particle images are located close to the center of the image.

The first assumption leads to a negligible error due to the fact that the shift angle $2\omega_m\Delta t$ is usually less than 0.1° . The relations $\sin(2\omega_m\Delta t) = 2\omega_m\Delta t$ and $\cos(2\omega_m\Delta t) = 1$ lead to the following formulae for the calculation of the particle image shift, when the formulae $1/f = 1/z_0 - 1/Z_0$ and $M = z_0/Z_0$ (see section 2.6.1) are used:

$$d_x(x, y) = \frac{x - M \cdot Z_m 2\omega_m \Delta t}{(x + X_m M) 2\omega_m \Delta t f^{-1} (1 + M)^{-1} + 1} - x \quad (4.2)$$

$$d_y(x, y) = \frac{y}{(x + X_m M) 2\omega_m \Delta t f^{-1} (1 + M)^{-1} + 1} - y. \quad (4.3)$$

These formulae are recommended for the practical use of image shifting by means of rotating mirror systems.

In many cases, the distance X_m from the mirror axis to the optical axis of the lens can be adjusted to zero. However, asymmetric configurations with X_m greater than zero allow the use of a smaller mirror.

The assumption that the particle images are located close to the center of the recording ($x \cong 0; y \cong 0$) leads to a systematic shift error in the measured displacement data. This error $\epsilon = (d_x - d_{\text{shift}}, d_y)$, which can be calculated when using equations (4.2) and (4.3), must be accounted for in the evaluation of PIV images. As an example, the difference between the local tracer image shift resulting from the mirror rotation, (d_x, d_y) , and the tracer image shift in the center of the observation field, d_{shift} , was calculated, given a set of typical experiment parameters: a magnification of $M = 1 : 4$, pulse separation, $\Delta t = 12 \mu\text{s}$, distance from the rotating mirror axis to the light sheet $Z_m = 512 \text{ mm}$, mirror speed $\omega_m = 62.8 \text{ rad/s}$, focal length $f = 100 \text{ mm}$. Figure 4.14 indicates that the image displacement increases to $200 \mu\text{m}$ at the edges of the recording with a shift of only $194 \mu\text{m}$ present at the center of the recording.

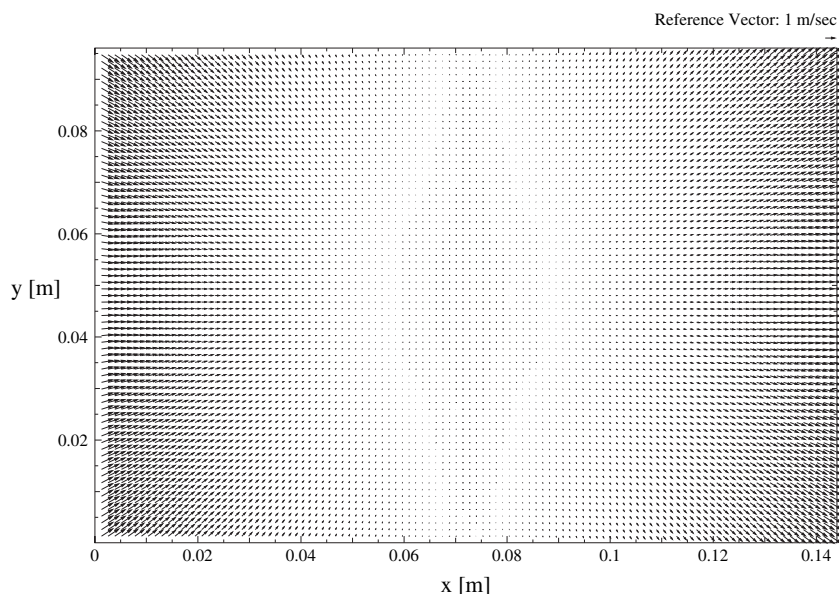


Fig. 4.14. Map of the calculated tracer image shift $(d_x - d_{\text{shift}}, d_y)$ due to perspective transformation.

4.3.6 Experimental Determination of the Mirror Image Shift

The error in the particle image shift on the PIV recording due to the use of a rotating mirror system for image shifting has also been determined experimentally. For this purpose PIV measurements were performed in air at rest. Tracer particles were injected into the air in the area of the observation field. The experimental setup is defined by the same parameters as given in the example calculation in the previous section. Particle motion resulting from convection and/or gravity effects was minor and therefore is negligible compared to the shift velocity of 64 m/s. Figure 4.15 displays the difference between the local tracer image shift and the tracer image shift in the center of the observation field. The scaling of the vector field is identical to figure 4.14.

The deviations between the experimental values and the theoretical values as calculated with equations (4.2) and (4.3) lie within the measurement resolution of our PIV evaluation system. Therefore we can safely assume that the rotating mirror-camera system was modeled correctly. The conventional practice – as described in the literature – of assuming that the value for the tracer image shift is constant over the entire image leads to systematic errors of 2–3% in the actual values of tracer image shift even for small observation angles. A virtual shift greater than the mean flow velocity is chosen frequently. This results in errors of up to 10% of the mean flow velocity. Equations (4.2) and (4.3) indicate that the shift of the particle images depends on the magnification, M ,

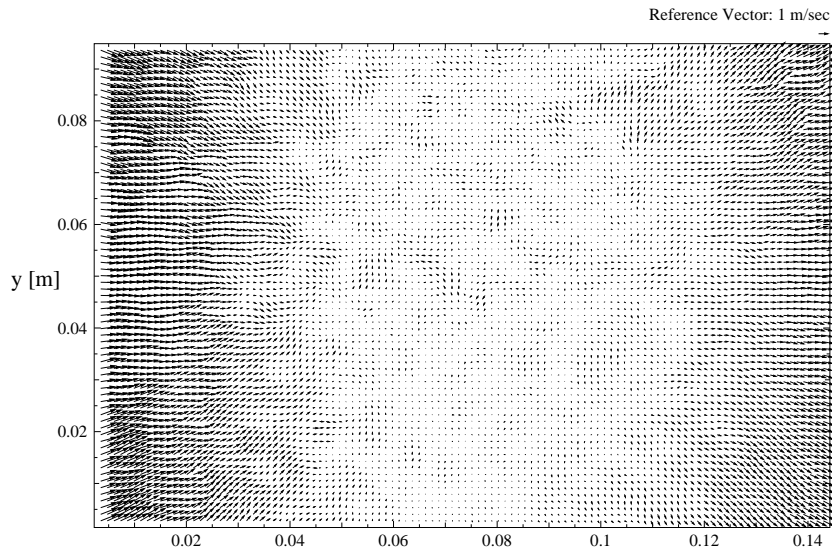


Fig. 4.15. Map of the experimentally determined tracer image shift ($d_x - d_{\text{shift}}$, d_y) of particles at rest on the recording. Same parameters were used for calculation and experiment.

the focal length of the lens, f , as well as the position of the mirror axis. These parameters stay constant during an experiment. Therefore, in order to be able to correct the measurement results appropriately, the locally varying tracer image shift has to be determined only once for a given recording configuration by means of the equations given above.

An alternative practical approach had also been implemented which avoids the need for an exact measurement of the parameters in equations (4.2) and (4.3). Usually after completion of the experiments, the fluid is left to come to rest while the shifting mirror continues to operate at constant angular speed. A PIV recording of the quiescent fluid ($U_{\text{residual}} \ll U_{\text{shift}}$) only records the effects of the image shift. By performing a second order least squares fit to the obtained virtual flow field, the distortions brought about by the mirror can be very well estimated and can subsequently be used to correct the actual PIV data of the original experiment. Such a direct calibration with subsequent fit to the expected function can also be used to analyze and compensate for the nonuniform image shift of other devices (e.g. nonuniform image shift by a birefringent crystal as reported by REUSS [105]).

Since the availability of the progressive scan CCD technology section 4.2, most PIV recordings are obtained in double-frame mode. However, ambiguity removal by means of image shifting might still be of interest if the cameras do not allow for frame transfer within the pulse separation time required.

4.4 Multi-Frame PIV Recording

In the following, a short summary of different techniques for multi-frame PIV recording is given. A more detailed description of the most frequently used video-based implementations of double frame/single exposure recording is presented in a subsequent section 4.4.1. The main advantages of separating the light of the subsequent recordings on to different frames have already been stated above: it solves the directional ambiguity, allows the adaptation of the pulse separation time in a wider range, and higher signal-to-noise ratios in the correlation plane are available at the same interrogation window size. In most cases, the improved signal-to-noise ratio will be used to compute the displacement within smaller interrogation windows and therefore increasing the spatial resolution at the same resolution of the recording.

Distinguishing the different illuminations could be done by coding the light sheets by different polarizations [88, 95], or by image separation using a color video camera and a color coded light sheet [87, 90, 91]. Both methods seem to be feasible in some situations, but because of additional optical problems associated with these methods they are no general solution. Depolarization due to glass windows and model surface scattering has to be considered as well as depolarization due to particles of larger size. First tests of the recording of small tracer particles in air with a two-color pulse laser system and color film already showed that the focal plane for green light can be displaced by up to 20 mm with respect to the focal plane for red light.

The separation of different exposures can also be performed by the timing of the image recording with respect to illumination. This can be done, for example, by means of high-speed film cameras in combination with copper vapor lasers [376] or multiple oscillator Nd:YAG lasers [107]. However, these experimental setups are very difficult to handle and are suitable only for special applications as for example for flow investigations in piston engines. More general solutions based on the proper timing of video cameras will be described in the following.

4.4.1 Video-Based Implementation of Double Frame/Single Exposure PIV

The low cost and frequent availability of standard video equipment and associated PC-based frame grabbers make their use for PIV especially attractive if spatial resolution is not of primary concern. In the following, three schemes capable of providing image pairs of single exposed particle image recordings are briefly described.

Mode 1: The first approach can only be applied to rather slow flows ($U_{\max} < 5 \text{ cm/s}$), which makes it useful only in water applications and is essentially equivalent to the original implementation of DPIV described by WILLERT & GHARIB [174]. As shown in the timing diagram in the upper part of figure 4.16, the laser light is strobed exactly in phase with the frame

rate of the camera. If a vertical synchronization pulse is not directly available from the camera, it may be obtained using a synchronization stripper. The duration of the light pulse from a continuous wave laser should not exceed one fourth the frame period (approximately 8 ms) to avoid excessive streaking of the particle images in the recording.

Mode 2: The second method of PIV recording based on video imaging utilizes the electronic shutter frequently available in today's video cameras. However, as mentioned before, these shutters generally work only on a field-by-field basis such that the recorded PIV images will have only half the vertical resolution. The interlacing nature of video can thus provide the user with video frames, each containing a PIV image pair. The odd video field (i.e. all odd lines) comprise the first PIV recording, while the even field (i.e. all even lines) correspond to the second PIV recording. The time delay between the recordings and hence the light pulse delay, Δt , is equal to the field interval of $1/50^{th}$ or $1/60^{th}$ of a second, which doubles the temporal resolution as well as the maximum recordable fluid velocity compared to **Mode 1** (figure 4.16, middle). Another advantage of this method is that the utilization of the electronic shutter allows continuous light sources to be used. The shutter time should be chosen to be long enough to allow the sensor to be exposed but short enough to avoid excessive streaking, typically less than one fourth of the field rate (e.g. 1/250 s). To process the digitized video frame, the user

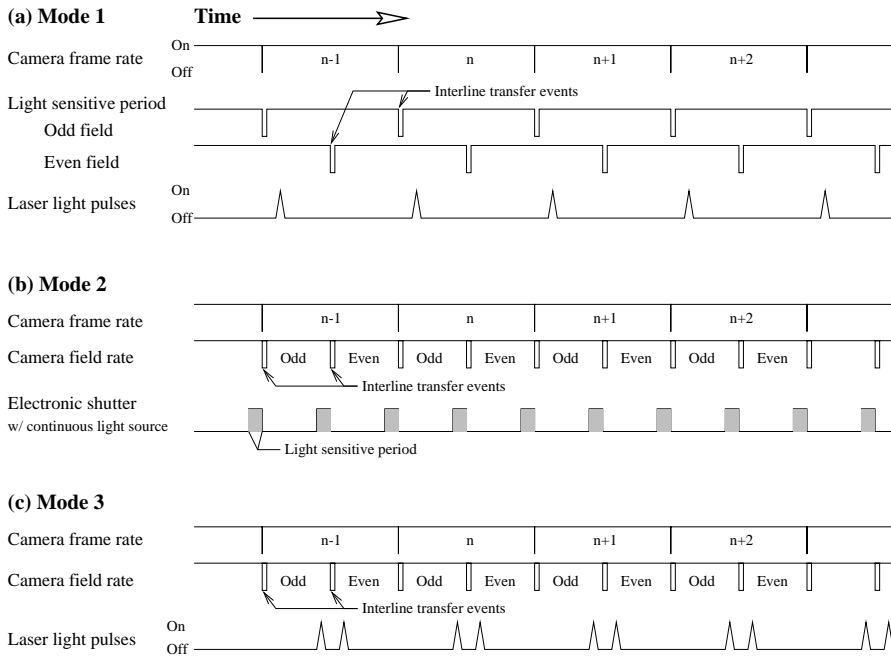


Fig. 4.16. Timing diagrams for PIV recording based on standard video equipment.

must first separate the interlaced image into an image pair, optionally also interpolating the missing lines of each image.

Mode 3: This approach is similar to the one above with the difference that no electronic shutter is used on the sensor and that the illumination pulses are provided asynchronously (i.e. *frame straddling* as described on page 106). This approach extends video-based PIV recording to provide images of high-speed flows [97, 100, 106]. The associated timing diagram is shown on the bottom of figure 4.16.